

FROM ORBITAL DEBRIS CAPTURE SYSTEMS THROUGH INTERNAL COMBUSTION ENGINES ON MARS

OLD DOMINION UNIVERSITY

S93-12
160609
P. 8

The investigation and conceptualization of an orbital debris collector was the primary area of design. In addition, an alternate structural design for space station *Freedom* and systems supporting resource utilization at Mars and the moon were studied. Hardware for production of oxygen from simulate Mars atmosphere was modified to permit more reliable operation at low pressures (down to 10 mb). An internal combustion engine was altered to study how Mars atmosphere could be used as a diluent to control combustion temperatures and avoid excess Mars propellant production requirements that would result from either methane-rich or oxygen-rich, methane-oxygen combustion. An elastic loop traction system that could be used for lunar construction vehicles was refined to permit testing. A parabolic heat rejection radiator system was designed and built to determine whether it was capable of increasing heat rejection rates during lunar daytime operation. In addition, an alternate space station truss design, utilizing a pre-integrated concept, was studied and found to reduce estimate EVA time and increase the structural integrity when compared to the original Warren truss concept.

An orbital-debris-capturing spacecraft design which could be mated with the Orbital Maneuvering Vehicle was studied. The design identified Soviet C-1B boosters as the best targets of opportunity in Earth orbits between an altitude of 900 km and 1100 km and at an inclination of 82.9°. A dual robot pallet, which could be spun to match the tumbling rate of the C-1B booster, was developed as the conceptual design.

INTRODUCTION

Students participated in six space systems design projects during the 1990-91 academic year. Design teams investigated alternate truss structure designs for Space Station *Freedom*; an orbital debris capturing unit; a locomotion system for lunar construction vehicles; a focusing radiator system for lunar heat rejection applications; production of oxygen from Mars atmosphere, and methane/oxygen-fueled engines for Mars applications. Mars oxygen production and lunar construction vehicle systems were continuations of previous design projects, while the other four projects were initiated during the present academic year. The participation of J. P. Raney, who was on loan from NASA Langley Research Center, is gratefully acknowledged.

The orbital debris capturing system and the space station truss designs were primarily paper studies, while the other four projects involved designing and building hardware that can be used to evaluate the specific design through further testing. The Mars oxygen processor assembly was rebuilt in order to eliminate leaks that have compromised earlier tests when conducted at subatmospheric pressures. The track system for a lunar construction vehicle has reached a design stage where its performance can be evaluated under simulated operating conditions. An internal combustion engine was modified to use methane fuel and pure oxygen, diluted subsequently with carbon dioxide, to study how stoichiometric methane-oxygen mixtures can be used for internal combustion engines on Mars. A focused parabolic collector system was designed and built to operate in a cryogenically cooled vacuum environment to investigate infrared heat rejection efficiency in the presence of a columnated sun-lamp heat source.

ORBITAL DEBRIS COLLECTOR

The population of objects in low Earth orbit (LEO) is currently monitored by the North American Aerospace Defense Command (NORAD). It catalogs and determines trajectories and orbital decay rates for all objects that can be observed and tracked by its ground-based radar systems. Currently, NORAD is capable of tracking objects as small as 4-10 cm in diameter. Those data show that the LEO environment is crowded with space debris. At this time, it is accepted that the population density of orbital debris is not yet prohibitive for spacecraft. However, this could easily change, particularly if any major collisions occur. A large effort has gone into determining the future amount and type of orbital debris. Even if no more launches were made, the level of orbital debris is expected to continue to grow from continuing collisions that generate more fragments. A literature search was conducted to determine primary types of debris and their population distributions to conceptualize the design of the debris collector. D. Kessler⁽¹⁾ has documented the growth and size of orbital debris in LEO and has targeted specific regions that need immediate debris removal. These regions are ranked by likelihood of impending collisions. The present design study has focused on developing methods for collection and removal of debris in regions that contain large objects in collisionally unstable orbits. By collisionally unstable, it is meant that the population density of objects of a particular orbital interval is sufficiently high that there is a significant probability of a self-sustaining series of collisions occurring from a single initial collision. The main reasons for the decision to target large objects are that large pieces of debris are relatively easy to capture and there is a dangerous potential for larger objects to dis-

integrate into millions of postcollision fragments. The exact regions of interest lie between altitudes of 700 and 1000 km, and between angles of inclination of 70° and 85°.

The debris in this region is largely of Soviet origin^(2,3). The initial target selection process focused on possible types of debris that could be collected. In this region the Soviets deploy three types of satellites: navigation, oceanographic, and ferret. Many of these satellites are accompanied by their associated spent second-stage booster rockets. Finally, there is a very large number of fragments that have been generated by these satellite programs. Evaluation of the debris types show that the second stage of the Cosmos C-1B booster has many features that argue for priority in cleanup. It is present in large quantity, it presents a very large target cross-section to possible debris collisions, and rocket bodies have the tendency to spontaneously explode due to failure of fuel tanks.

An in-depth survey showed that the population of orbiting Cosmos C-1B second-stage boosters was sufficiently high to justify them as a specific target for removal. There are 59 Cosmos C-1B rocket bodies at an angle of inclination of 82.9°. Their distribution at this angle of inclination over various altitudes is shown in Fig. 1.

Restricting attention to C-1B boosters, the problem is determining exactly what type of motion the orbiting booster might possess. J. Turner of NASA Marshall Space Flight Center provided results from a Martin Marietta Corporation study⁽⁴⁾ that determined that these bodies evolve rapidly to a rotational motion about their major axis (principle moment of inertia), as shown in Fig. 2. It was also determined that uncontrolled bodies in LEO will typically have rotation rates of up to 7 rpm, which dictated the design requirements for this study.

To intercept a rotating body in space, a conceptual orbital debris collector (ODC) kit was developed that was to be mounted aboard the orbital maneuvering vehicle (OMV). The OMV was assumed to provide all power, tracking, and orbital transport needs, placing further limits on the present design. The two main features of the current kit are its spin table and arm/cradle assemblies. The required spin table was a flat circular plate 14' in diameter and 1" thick. It provided the rotating

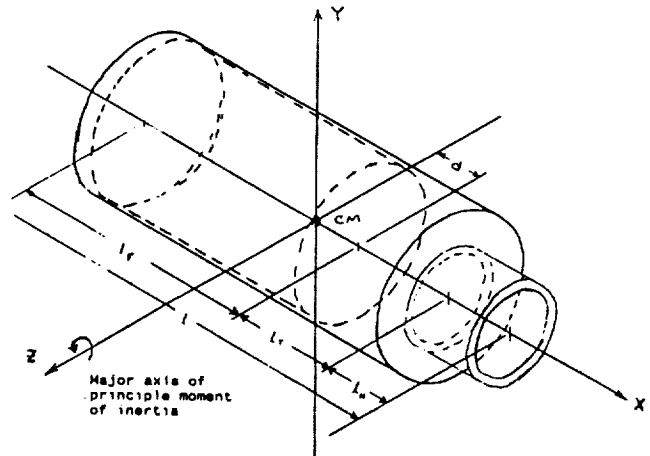


Fig. 2. Rotational motion of rocket bodies in low Earth orbit.

base for the robotic retrieval arms. The current design utilizes a DC motor to provide the torque required to adjust the spin table's angular velocity to that of the rotating rocket body. Also included in this design, for purposes of postcapture deceleration, is a compressed gas diaphragm brake mechanism. The brake mechanism has been designed to stop all rotational motion of a captured Cosmos C-1B within five minutes of brake initiation. The other main components of the ODC kit are the robotic arms and cradles. Figure 3 shows a three-dimensional CADAM graphic illustration of the proposed conceptual kit. The arms were analyzed through the use of NASTRAN. Aluminum tubing with an outer diameter of 8 cm and an inner diameter of 6 cm was chosen as the construction material for the structure. The chosen dimensions provided a large factor of safety in terms of the estimated applied load.

A complete mechanisms analysis was performed to determine a configuration that could exhibit rectilinear motion. The ability to perform rectilinear motion was deemed important because

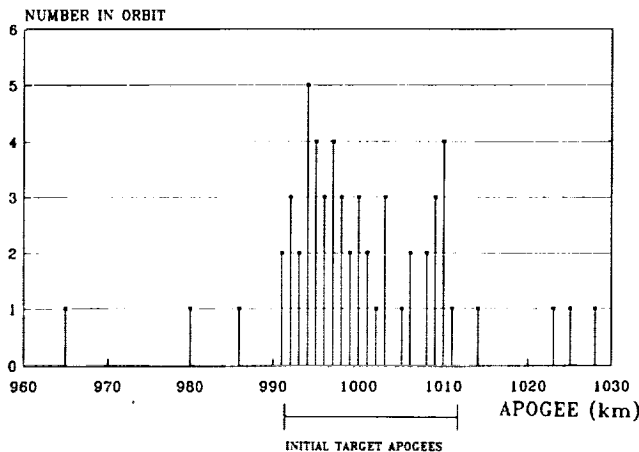


Fig. 1. Distribution of Cosmos C-1B rocket bodies.

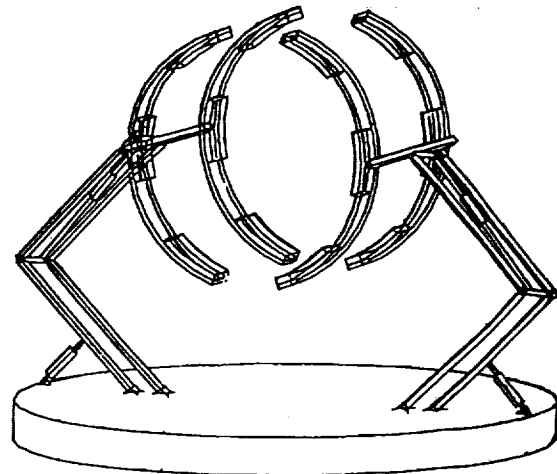


Fig. 3. Conceptualized orbital debris collector.

it would free any operator or operating system of anticipating the final landing point. Errors at this phase of operation could result in setting the body into chaotic motion, thus destroying the ODC/OMV assembly. For the rectilinear motion a double four-bar mechanism was selected. The motion of this mechanism is to be controlled by linear motor actuators, for which position and velocity requirements have been computed. It is important to note that the cradle dimensions were sized specifically for the C-1B, and that soft contact pads are to be placed, as shown in Fig. 3, on the cradles to minimize contact jarring.

Several calculations of velocity change necessary to deorbit the captured debris proved the feasibility of an OMV/ODC disposal mission in terms of requiring OMV performance levels well within the capabilities of the OMV thrusters. However, more work is needed to determine exact fuel requirements and mission utility limits. Sample missions were outlined to demonstrate the various stages and modes of operation required for particular missions. More important features of these sample missions included the use of the space shuttle for deployment of the assembled OMV/ODC and the use of a matched orbital velocity for initial approach to minimize plume impingement.

Future work on this project should include optimizing the configuration of the arms using more advanced materials, such as Kevlar or Spectra Fiber. More orbital mechanics must be done to obtain more precise data on fuel consumption and ranges of missions. It is also recommended that an experimental program be set up to determine structural loads and control system performance at rendezvous as well as to study the effects of misaligned interceptions.

SPACE STATION TRUSS DESIGN

While NASA has been working on Space Station *Freedom* designs for over 10 years, they have been plagued by budgetary constraints. Recent budget problems have forced NASA engineers to look for alternative designs. Since the basic truss structure is a key element in any space station design, the purpose of this project is to define an alternative truss design for the space station and compare it with the original one. The alternative design had to meet the functional requirements established by NASA and by congressional mandates.

The functional requirements are mission oriented. The truss structure must serve as the backbone of the station and secure the habitat and laboratory modules. It must carry the photovoltaic (PV) arrays that provide power to the crew and scientists aboard the station. Also, the truss structure must have an effective life of at least 30 years and be capable of withstanding a catastrophic failure of a single member. Therefore, the truss structure must maintain the structural and geometric stability of the station as a whole. Congress has determined that the space station should be easily assembled in space and has dictated that the cost be much less than estimated originally. Therefore, this design group has studied an alternative truss structure design concept that satisfies the functional requirements mentioned above and addresses the congressional mandates. As seen in Fig. 4, the alternative design employs an eight-sided regular polygon with a nominal 4 m diameter (between opposite sides). Each octagonal element is separated by 1-m truss members and diagonal stiffeners opposite in direction along the surface.

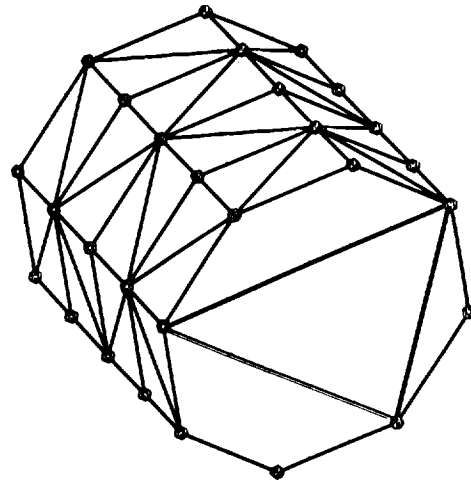


Fig. 4. Schematic of basic structural element for alternative design.

Internally, a triangular truss assembly provides additional stiffness. Each internal triangular stiffener is placed longitudinally, every 4 m. Overall, the alternate design is cylindrical and approximately 100 m long. The truss is assumed to carry three PV arrays and several habitat/laboratory modules as shown schematically in Fig. 5. Each shuttle flight will deliver a 12-m long, preassembled section of the station. This assembly approach reduces dramatically the amount of time required to construct the station in orbit. It was estimated that 17 shuttle flights will be required to deliver all sections of the space station truss to LEO.

Analysis of the alternative design was performed using NASTRAN/PATRAN. The design was compared to the original space station truss design for evaluation. A Warren-type truss was implemented in the original or baseline design. The

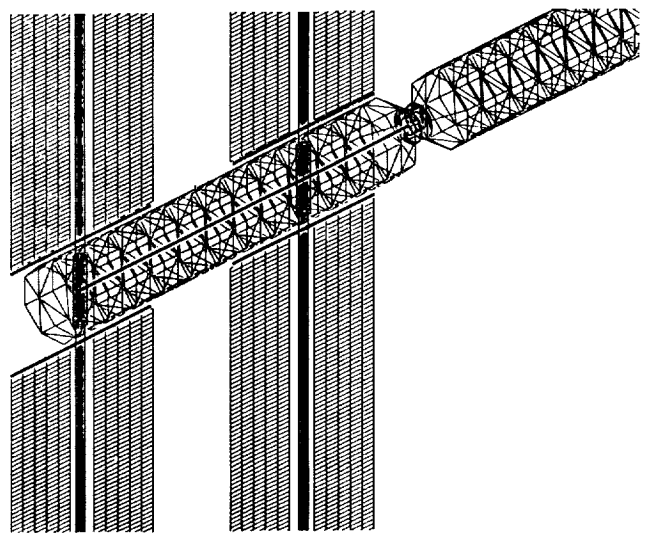


Fig. 5. Schematic of structural module attached to solar array.

deflection estimates, obtained from a static analysis, showed that the alternative truss was superior to the original design. Vibrational results of the design have not been finalized yet. Therefore, additional work should be performed on the vibrational characteristics of the alternative space station truss. The estimated number of shuttle flights required for the alternative design was approximately half that required by the original design and less time was required to construct the preassembled truss, thus reducing the total EVA time.

ELASTIC LOOP TRACK DESIGN

An Elastic Loop Mobility System (ELMS) design was selected as the traction system for Old Dominion University's 1990 Lunar Construction Utility Vehicle (LCUV) design⁽⁵⁾. The concept was studied previously by Lockheed Corporation⁽⁶⁾ for use on a Mars explorer vehicle. The goal of the 1991 design group was to evolve the ELMS hardware sufficiently to enable testing and evaluation.

The ELMS combines the traction capabilities of tracks with the light weight and relatively low power consumption of wheels. The ELMS employs an elastic loop that grips the lunar soil in a manner similar to a traction chain on a bulldozer. Unlike a chain-link track, the elastic track was made of a single band of material shaped in a loop. In addition to transporting the body of the vehicle, the ELMS protected the instrumentation of the LCUV. The two loops also assisted in the suspension of the LCUV by suspending the drive drums above rocks and other obstacles that would otherwise jar the vehicle.

As can be seen in Fig. 6, the elastic loop rides on two drive drums. Tension on the loop is supplied by the spring assemblies that are mounted onto pivot plates. Two rollers on each loop-wheel assembly provide guidance and aide in keeping proper tension on the loop. A 22-gauge, type-304 stainless steel sheet was selected for elastic loop construction. Unfortunately, the thickness chosen was too thin to suspend the vehicle as desired. However, the modified suspension system had attributes appropriate for further testing.

The suspension system must maintain proper tension on the loop and dampen vibrations. Proper operation of a suspension system prevents shock loads from reaching the hull of the LCUV.

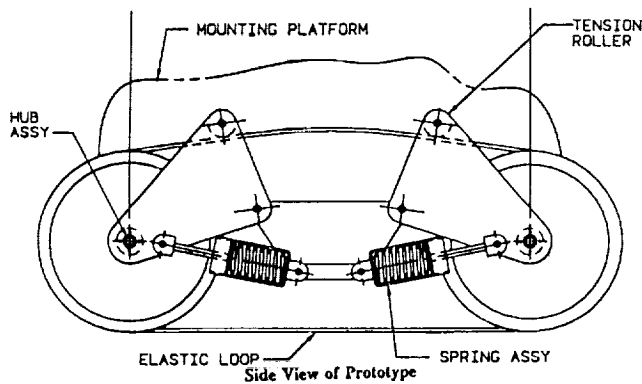


Fig. 6. Side view of elastic loop track system.

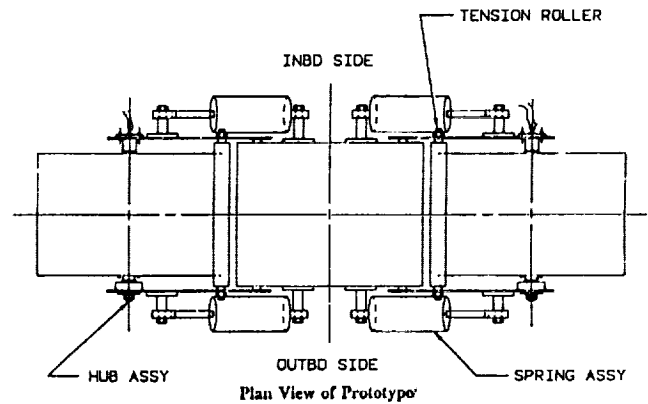


Fig. 7. Plan view of elastic loop track system.

This is accomplished by the utilization of four spring assemblies on each loopwheel as seen in Fig. 7. A close-up view of a spring assembly is shown in Fig. 8. If the spring constant, κ , is low the springs will allow pitching motion of the vehicle in starting and braking situations. Springs with higher κ values have a higher energy absorption ability than the softer springs, but little cushioning effect⁽⁷⁾.

Several assumptions were made in the design of the spring/suspension assemblies. These assumptions involved lunar temperature fluctuations and the lunar dust/soil problem. The nature of the lunar environment poses many problems for the design of an LCUV. The lunar day lasts 27.3 days with approximately two weeks of sunlight and two weeks of darkness. In addition, the surface temperature can range from 374 K during the lunar day to 120 K during the lunar night⁽⁸⁾. These temperature fluctuations will cause subsequent expansions and contractions of the spring assemblies, thus changing the tolerances. The first assumption, therefore, is that lunar temperature fluctuations will not affect tolerances. Ground laboratory studies of lunar soil samples from different regions of the lunar surface have shown that the mechanical properties of the upper layer of the lunar soil can vary over a wide range and depend on both the depth of the upper fine-grained layer and the degree of packing⁽⁹⁾. Final designs must protect the suspension system from lunar dust.

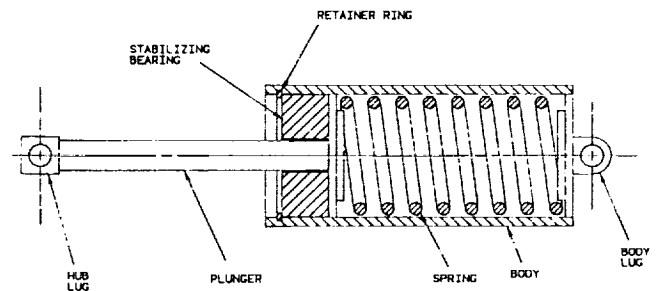


Fig. 8. Schematic of spring assembly.

The spring system incorporates coulomb damping as a method to reduce vibration. In coulomb damping, dry sliding friction forces dissipate energy from a vibrating system by opposing the motion between two members in contact. In the present case, relative motion between the plunger and body of the spring assembly is responsible for frictional damping. The energy dissipated in damping causes the magnitude of the vibration to decrease continuously until the system comes to rest.

Eight spring assemblies (four per loopwheel) were required for a complete traction system. They were attached on an adjustable track to allow them to be oriented in different directions. A loosely fitted loop would require the spring assemblies to be mounted further apart than when they were located on a tight loop. Other items used to maintain tension on the loop were the tension rollers (see Fig. 7). In order to guide the loop across the suspension system, two rollers were scheduled to be mounted onto each loopwheel. However, testing of different materials for the loop demonstrated that the rollers were not required for the stainless steel loop. When necessary, the rollers and the spring assemblies could be attached to the pivot plates to provide a balanced system.

Direct current motors were used on the ELMS for both propulsion and steering. Each loop utilized two 90-V motors that were synchronized in both rotational speed and direction. By varying the voltage between the motors, thrust could be varied between the two loops. Thus, a moment would be created that, in effect, turned the vehicle when the loops were driven in opposite directions.

The drive motors were encased in individual drive hubs to prevent lunar particles from interfering with their performance. Though variances in loop thrust were desirable for turning the vehicle, variances in motor rpm were not. Unsynchronized motors tended to imbalance the vehicle by pivoting the body forward or backward. Such a condition strained the other motors, sometimes to the point of shearing keys along the motor mounts.

In summary, an overall system design has been produced that can be used to test propulsive performance and steering. Although the 22-gauge stainless steel loop is less rigid than desired, the loop system still exhibits sufficient elasticity and damping to warrant further testing.

PARABOLIC REFLECTOR

Recently, Costello and Swanson⁽¹⁰⁾ proposed a lunar radiator design that incorporated a flat, two-sided radiator with a specular, parabolic reflector. Their analysis showed that if the edge of the rectangular radiator were on the symmetry plane of the reflector and its upper edge terminated below the focal line (Fig. 9), improved lunar-daytime heat rejection could be accomplished when the reflector tracked the Sun. A system was built to test their predictions.

A cylindrical vacuum chamber (12" diameter by 12" high) was built that could accommodate a parabolic reflector with a 6" × 8" aperture. The focal length of the reflector was 2.5" and the infrared radiator unit was constructed as a sandwiched, electrically heated 2" × 6" plate. Solar heating was simulated using a sun lamp that was columnated through a Fresnel lens. Both units were located outside the vacuum chamber above a window located in the chamber's top surface. The inner

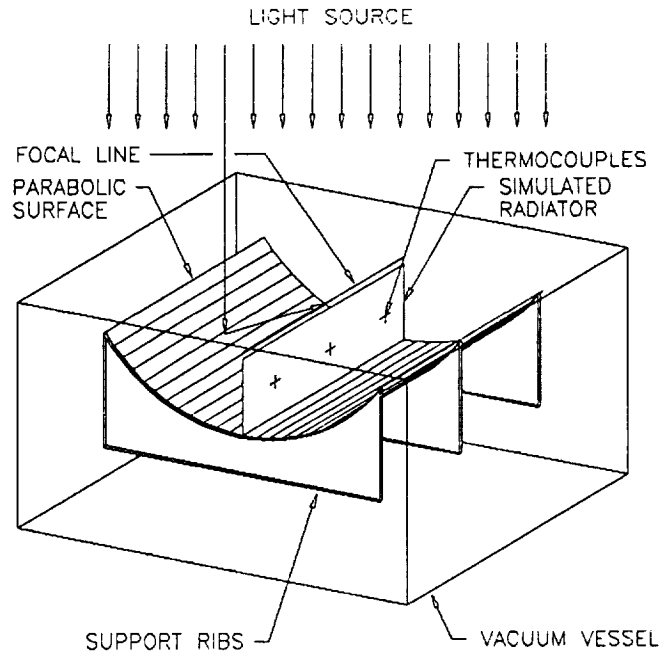


Fig. 9. Schematic view of radiator-reflector experiment.

surfaces of the vacuum chamber were coated with flat black paint and the cylindrical chamber wall was cooled using liquid nitrogen to simulate deep space.

The reflector contour was cut from wood using a numerically controlled milling machine and the reflector surface was produced using a thin layer of Kapton coated with vacuum-deposited aluminum. The infrared heater-plate was coated with flat black paint and a thermocouple was epoxied between the plates and the inner resistive heating element.

Preliminary tests were conducted that measured the transient rate at which the reflected and unreflected radiator was heated and cooled in the presence of the simulated solar heat source. Both sets of measurements showed that the reflected radiator was more efficient than the unreflected unit. However, the tests were not performed with adequate control to permit anything but qualitative interpretation. It is anticipated that an upgraded version of this system will be developed in time for the 1992 conference.

METHANE ENGINE OPERATION ON MARS

If carbon dioxide and water are the feedstock ingredients for propellant production systems on Mars, methane and oxygen are the logical products. A fully operational chemical plant will produce a stoichiometric mix of methane and oxygen products and the energy required to produce those should be minimized. As a result, a dedicated propellant plant is most efficient when oxygen and methane are used in stoichiometric proportions. However, engine combustion temperatures are excessive for stoichiometric combustion, a noncombustible diluent is preferred to either fuel-rich or oxidizer-rich combustion to avoid wasting methane or oxygen. A logical diluent on Mars would

be unprocessed Mars atmosphere. Depending on the engine operating conditions, the atmospheric gas could be mixed using either a "supercharger" or by carrying precompressed gas. Regardless of the form of supply, questions concerning the range of acceptable levels of carbon dioxide for efficient engine operation should be addressed. Under what operating conditions are performance and operability requirements met without resulting in significant carbon buildup or without causing other processes to occur that limit engine reliability, maintainability, or performance?

A Megatech Mark III laboratory engine was modified to use gaseous methane, oxygen, and carbon dioxide as the fuel and oxidizer mixture. The original unit was a 4-stroke, 0.5-horsepower (370 W) engine, using methanol. The unit was modified so that gaseous fuel, oxidizer, and carbon dioxide were supplied through independently valved lines, and each flow was monitored via rotometers, as shown in Fig. 10. The compression ratio of the engine could be varied between 3 and 4. Preliminary tests were conducted operating the engine at 3:1. Typical engine performance curves for a mixture of 0.25 CH₄, 0.5 O₂, and 0.25 CO₂ are shown in Figs. 11 and 12.

Unlike a liquid-fueled, air-oxidizer engine, the pressurized fuel and oxidizer were capable of providing some work via the pressurization of the cylinder. Hence, the performance of the engine was corrected by deducting the amount of work that could be extracted via adiabatic expansion of the propellant products.

Initial tests showed that the engine did not operate in a "steady-state" mode in the sense that the crank shaft speed (rpm) varied cyclically during controlled fuel-oxidizer supply operation. The cyclic behavior was also observable via changes in the color of the combusting gases (which could be monitored through the glass cylinder wall). Further testing is required to establish operating envelopes for Mars applications.

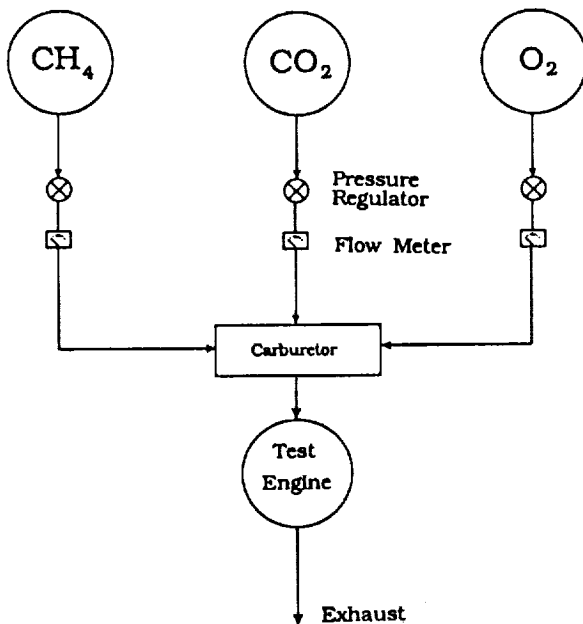


Fig. 10. Schematic of gas supply system for engine tests.

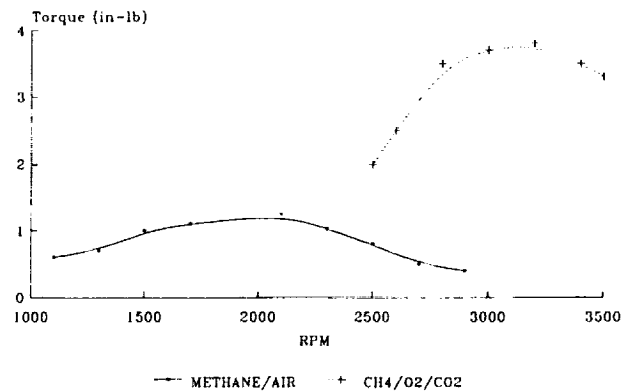


Fig. 11. Comparison of engine torque performance for methane/air combustion with CH₄, CO₂, 2O₂.

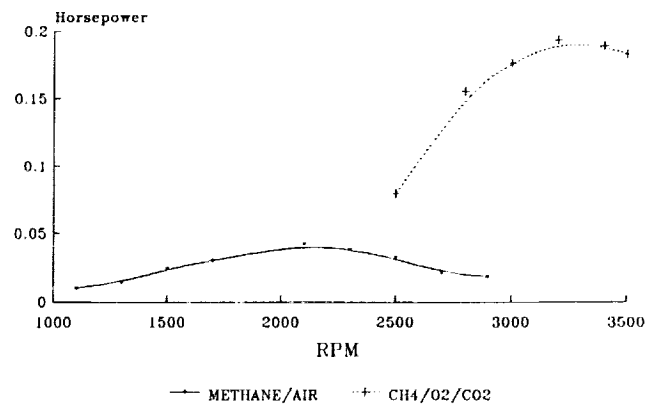


Fig. 12. Comparison of engine horsepower performance for methane/air with CH₄, CO₂, 2O₂.

MARS OXYGEN PROCESSOR

Production of oxygen from Mars' atmosphere was identified in 1979 as an early opportunity for extraterrestrial resource utilization at Mars⁽¹¹⁾. Subsequently, a demonstration system was designed and built with support from the Planetary Society and USRA that produces oxygen from simulated martian atmosphere⁽¹²⁾. Operation and evaluation of that system has continued to evolve, but difficulties have been experienced in performing tests below 1 bar pressure. Air leaks have compromised the experiments performed at simulated martian operating conditions. A design group was charged with evaluating the instrumentation and system piping to determine how to eliminate leaks and modify the instrumentation to measure system performance more accurately.

The present Mars oxygen processor system is shown schematically in Fig. 13. Testing showed that the original piping layout had employed three types of stainless steel tubing with leaks produced from one tubing type. In addition, the procedure

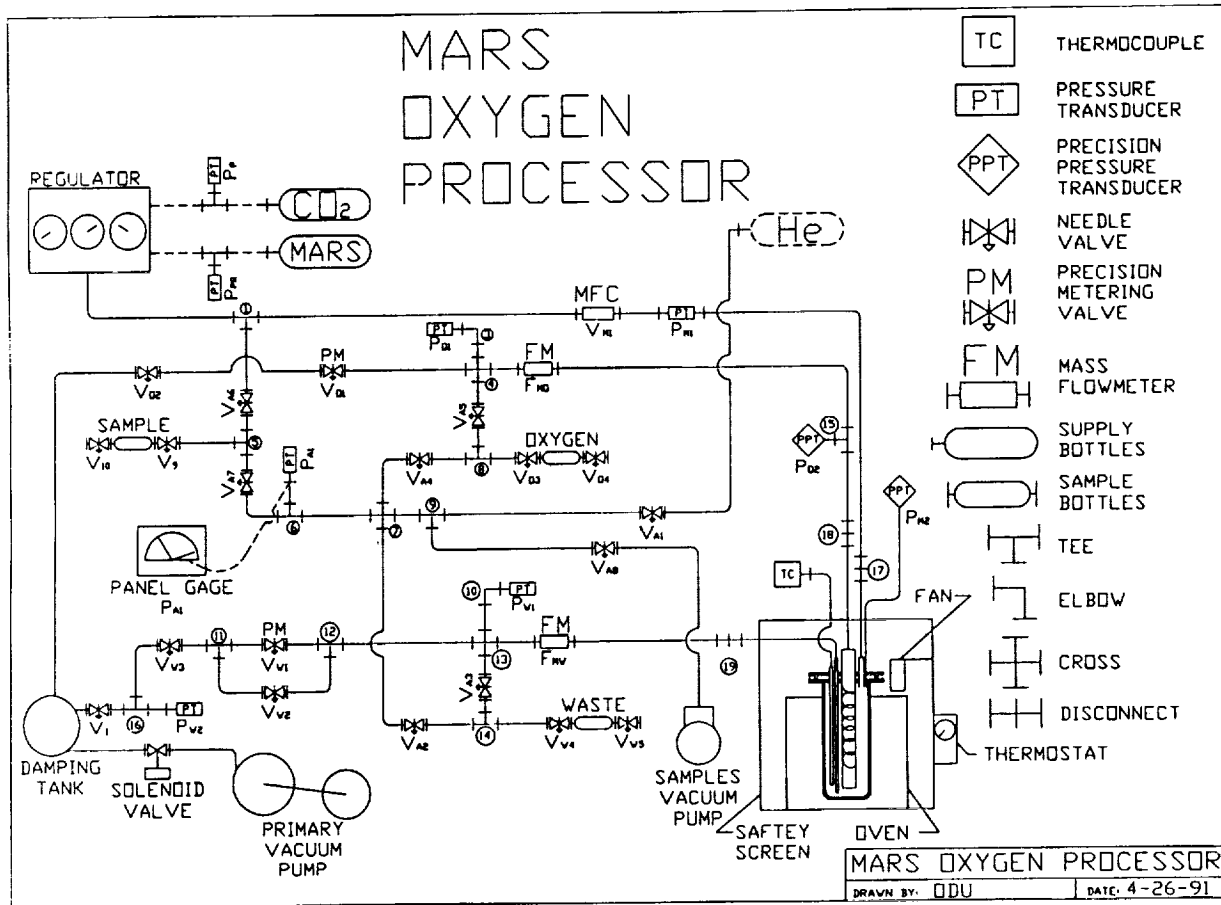


Fig. 13. Schematic of Mars oxygen processor layout.

used to disassemble and reassemble the tubing connections produced leaks. Tubing was standardized and procedures were developed to control the system assembly process. A procedure was also developed that enabled the pressure transducers, employed throughout the layout, to be checked periodically against a calibrated reference source. While these aspects of the system design were tedious (including discovery of a programming error in reading temperature via the data acquisition system), the oxygen processor unit is now capable of low-pressure operation. Tests will be run during the summer of 1992.

CONCLUSIONS

Students have engaged in space system design projects ranging from conceptual design of an orbital debris capture system through developing procedures to improve measurement quality for operational hardware. The space debris capturing strategy is both novel and worthy of further consideration by NASA. A specific orbital volume 82.9° inclination, 1000 km altitude contains 59 spent Soviet C1-B rocket bodies. The hardware-oriented projects have all evolved toward producing useful systems that can ultimately lead to publication-quality results.

REFERENCES

1. Kessler D. J. (1989) Current orbital debris environment. In *Orbital Debris from Upper Stage Breakup* (J. P. Loftus Jr., ed.). *Prog. Astronaut. Aeronaut.*, 121, 2-12.
2. King-Helle D. G. et al. (1987) *The RAE Table of Earth Satellites (1957-1986)*. Stockton Press, New York.
3. NASA Office of Public Affairs (1991) *Satellite Situation Report*, Vol. 27, No. 4, NASA Goddard Space Flight Center, Greenbelt, Maryland.
4. Cable D. A. et al. (1986) *Concept Definition Study for Recovery of Tumbling Satellites, Vol. 1. Executive Summary*, Martin Marietta, Denver Aerospace Division, Contractor Report MCR-86-1329, (NASA Contract NAS8-36609).
5. Old Dominion University. (1990) Design of an autonomous lunar construction vehicle. In *Proc. 6th Annual Summer Conference*, pp. 169-173. NASA/USRA University Advanced Design Program, NASA Lewis Research Center, NASA CR-187041.
6. Trautwein W. (1972) *Design, Fabrication and Delivery of an Improved Elastic Single Loop Mobility System (ELMS)*. Lockheed Missiles and Space Co., NASA Contractor Report NASA CR-123841.
7. Hohl G. H. Torsion-bar spring and damping systems of tracked vehicles. *J. Terramechanics*, 22, pp. 195-196.
8. *The Lunar Split Mission: A Robot Constructed Lunar Base Scenario*, Summer Design Report for the NASA/USRA Advanced Space Design Program, p. 62. NASA Johnson Space Center.
9. Lenonovich A. K. et al. (1972) Investigations of the mechanical properties of the lunar soil along the path of Lunakhod 1. *Space Research XII*, Akademic-Verlay, Berlin.

10. Costello F. A. and Swanson T. D., (1990) *Lunar Radiators with Specular Reflectors*. AIAA/ASME 5th Joint Thermophysics and Heat Transfer Conference, Seattle, Washington.
11. Stancati M. L., Niehoff J. C., Wells W. C. and Ash R. L., (1979) *Remote Automated Propellant Production: A New Potential for Round Trip Spacecraft*. AIAA Conference on Advanced Technology for Future Space Systems, NASA Langley Research Center, AIAA Paper No. 79-0906.
12. Ash R. L., Werne J. A., and Haywood M. B., (1989) pp. 479-487. Design of a Mars oxygen processor In *The Case for Mars III*, (C. Stoker, ed.), AAS Science and Technology Series, 75.